JNPC Journal of Nasopharyngeal Carcinoma

Research Article

Optical Coherence Tomography for Quantitative Diagnosis in Nasopharyngeal Carcinoma

Jianghua Li[1], Jia Chen [2,*], Xiaojiang Mu[1]

[1]School of Mechanical and Electrical Engineering, Shenzhen Institute of Information Technology, Shenzhen, 518172, China.

[2]Department of Nephrology, Shenzhen Second People's Hospital, Shenzhen Second Peoples's Hospital, Shenzhen 518037, China.

[*]**Corresponding author**: Dr. Jia Chen, Department of Nephrology, Shenzhen Second People's Hospital, Shenzhen Second Peoples's Hospital, Shenzhen 518037, China. Email: lijianghua25@163.com.

Citation: Li J, Chen J, Mu X. Optical Coherence Tomography for Quantitative Diagnosis in Nasopharyngeal Carcinoma. J Nasopharyng Carcinoma. 2017; 4(6): e40. doi:10.15383/jnpc.40.

Competing interests: The authors have declared that no competing interests exist.

Conflict of interest: None.

Abstract: We tried to quantitatively diagnose the intrinsic differences in the optical properties of nasopharyngeal carcinoma from normal tissue by optical coherence tomography. The scattering coefficients and anisotropies are extracted by fitting the average a-scan attenuation curves based on the multiple scatter effect. The median scattering coefficients of epithelium are 2.2 mm^{-1} (IQR 1.5 to 2.5 mm^{-1}) for normal versus 3.8 mm^{-1} (IQR 2.0 to 3.3 mm^{-1}) for cancer tissue; of lamina propria are 2.9 mm^{-1} (IQR 1.5 to 2.5 mm^{-1}) for normal versus 1.3 mm^{-1} (IQR 1.2 to 12 mm^{-1}) for cancer tissue; and anisotropy factors of epithelium are 0.91 (IQR 0.9 to 0.93) versus 0.91 (IQR 0.88 to 0.97) for normal and cancer tissue; of lamina propria are 0.98 (IQR 0.94 to 0.99) for normal versus 0.98 (IQR 0.96 to 0.99) for cancer, respectively. The results show quantitative values of scattering coefficients combined with the morphological by optical coherence tomography can improve the diagnosis rate of nasopharyngeal carcinoma.

Keywords: Optical coherence tomography; Nasopharyngeal carcinoma; Scattering coefficients; Anisotropy; Quantitative

Introduction

Nasopharyngeal carcinoma (NPC) is a common head and neck cancer in South China, with an incidence of 15–50 per 100 000 people[1]. It is often called “Canton Tumor” because the highest morbidity of NPC in Guangdong Province, China. More than 70% of NPC patients have already developed cervical lymph node metastasis at initial diagnosis[2]. Given the unclear etiology of NPC, primary prevention remains difficult, and the main strategy for reducing NPC mortality is to identify the disease at an early stage[3]. Nowadays, the diagnosing NPC rely on histological and cytological examination of the biopsies, which have to be fixed and stained before diagnosis. Furthermore, NPC easily spreads to the lymph nodes and distant organs, most patients are diagnosed only when the tumor has reached an advanced stage (stages III and IV)[4]. Thus, a rapid, accurate and non-destructive technique may enable an earlier diagnosis of NPC is needed.

Optical coherence tomography (OCT) is a low coherence interferometric technique capable of label-free, noninvasive and depth-resolved imaging of tissue up to 1–2 millimeter below the tissue surface with micrometer-scale spatial resolution[5]. So, visual inspection of OCT images may be used to assess tissue morphology, which has been used in various fields, such as ophthalmology, dermatology, cardiology, dentistry, and cancer structure[6,7]. For example, several characteristics of OCT images can be used to differentiate between cancerous and normal tissues. In highly scattering tissues, OCT is sensitive to the disruption of normal tissue architecture or morphology (*e.g.*, layer thickness or scattering regularity), which is often associated with carcinomas[8,9]. The relative strength of the optical scattering[10] and attenuation[11] in OCT images provides another parameter to differentiate normal from cancerous tissues. Joint spatial frequency and textural image analysis, which is sensitive to speckle patterns as well as tissue architectural features, can also provide distinction between cancerous and normal tissues[10–12]. Nevertheless, the OCT yields only detailed information about the morphological features of tumor and doesn’t allow precise determination of cancer type. As a rule, the diagnostic sensitivity and specificity of OCT doesn’t exceed 75%–85% for different types of cancer. Moreover, the high sensitivity (about 85%) is accompanied with low specificity (60%–70%)[13].

Thus, the more accurate calculation method is developed. The research of quantitative determination using OCT has been reported[14–17]. And this improvement can identify the types which are not recognized by OCT structure. In which the scattering coefficient, absorb coefficient and anisotropy can be fitting from the OCT imaging. In this paper, multiple scattering effects are applied to determinatively the scattering coefficient and anisotropy of the normal and cancer tissue to test whether the quantitative method using OCT imaging can be used to diagnosis the NPC.

Materials and Methods

Patients and Tissue Sample

A total of 5 pieces of nasopharyngeal tissues and 5 pieces of NPC tissue were collected from 10 patients who underwent endoscopic biopsies. Each biopsy specimen was divided into two parts (with dimensions 1 cm×1 cm), one fixed in 10% formalin solution used for histopathologic examination and another used for OCT measurements. The histopathologic examinations were conducted by a specialist nasopharyngeal pathologist. Informed consent was obtained from all patients before the collection of surgical biopsy specimens. The longitudinal section of the histological nasopharyngeal mucosa and NPC are shown in Ref [18].

OCT System

The schematic diagram of our spectral domain OCT system used to perform images was previously reported[19]. The light source was a super luminescent diode with a center wavelength of 830 nm of approximately 40 nm and an axial resolution of 7.6 μm in air. The light that entered the source arm was split equally into the

JNPC Journal of Nasopharyngeal Carcinoma

reference and the sample arms of the Michelson interferometer, and then the interference signal of the light beams reflected from the reference and sample arms was coupled in the detection arm. As a low-coherence source was used, the light from the corresponding sample and reference arms only coherently interfered when their path lengths were matched to within the short coherence length. The detection arm consisted of an achromatic collimating lens (CM: f = 75 mm), a 1200-line/mm transmission grating, an achromatic focusing lens (FL: f = 200 mm). The integration time of the CCD camera was set to be 40 μs and the system was operated at a-scan frequency of 20 kHz. The output power of the sample arm was 0.5 mW. Data acquisition was implemented in Labview software (National Instrument, Austin, TX, USA).

Calculation of the Optical Parameters

According to the extended Huygens-Fresnel principle, multiple scattering effects have been taken into account, and thus the depth profile of the a-scan signal is a function of the scattering (μ_s) and absorption coefficient (μ_a) as well as anisotropy (g). The details of this model have been described by Levitz[14–17]. In brief, the algorithm consists of several steps: first, the transverse region of interests (ROIs) with thirty curves fitting attempts per ROI from every de-background image is selected; then these adjacent a-scans are averaged along the lateral direction to yield an attenuate curve, where the fitted length is chosen to be 0.23 mm (80 pixels). Finally, the parameters of the scattering coefficient μ_s, the root-mean-square scattering angle θ (g=cos(θ)), and error estimates are outputted. (Absorption coefficient could be neglected at 830 nm.) The first criterion in choosing is whether or not the best fit values of the parameters, and dependency, are physically reasonable. Ensemble averages and standard deviations of the fitting parameters of the values μ_s and g, were carried out with the Matlab software (The Mathworks, Inc., Natick, MA, USA), version 7.5. For all analyses, the errors less than 0.01 are considered. In all, twenty imagines with 5 ROIs (100 a-scans curves) are used for analyses.

Results

The representative cross-section OCT images of normal and NPC tissue are described in Fig.1, respectively. The intensity images range from black (background) to yellow (strong backscattering), then a color bar represents the attenuated backscattering light when it goes through the tissue. In which the normal stroma appears three layers: the epithelium, lamina propria, and basement membrane, the latter connects with the epithelium and lamina propria; while the level constructions of mucosa are destroyed by the presence of malignancy. The similar results are described in Ref [18].

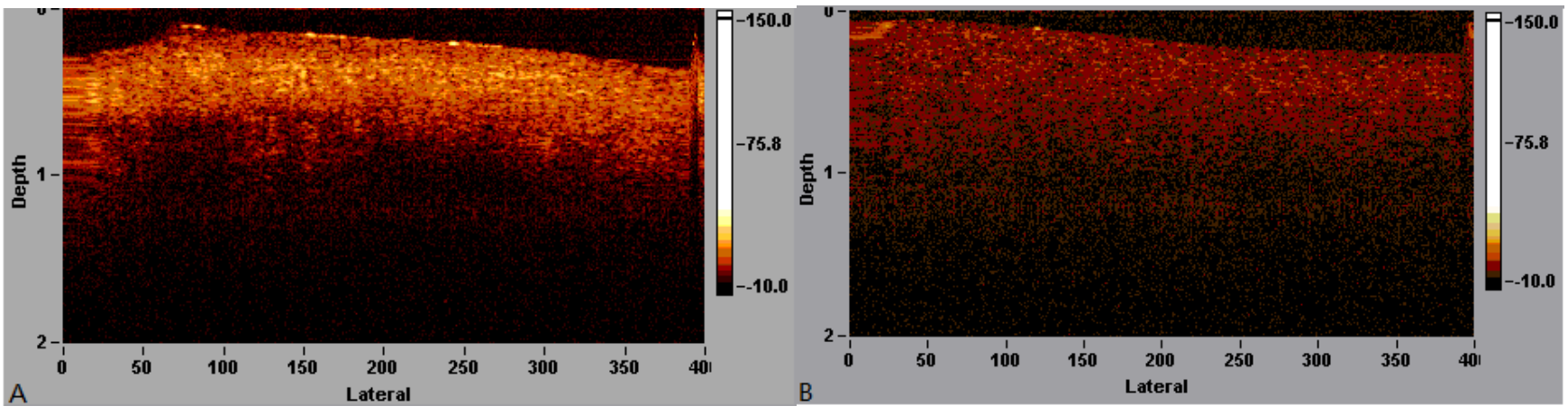

Fig. 1: The representative cross-section OCT images of normal (panel A) and NPC tissue (panel B).

The averaged a-scan lines from normal and cancer tissue fitting by 350 pixels region of the decay slope are displayed in Fig.2, respectively, shown by the intensity vs scan depth (pixels). Fig.2A shows that the slope in the level of epithelium increases as the function of depth, suggesting that the multilevel scattering is getting stronger. The intensity attenuates as the function of depth

show an exponential decay for lamina propria; the attenuate at the bouDndary is irregular. Fig.2B has the similar shape with Fig.2A except for basement membrane, which are consistent with the image of OCT.

The representative plots of fitting scattering coefficient and anisotropy factor from certain region of interest (ROI) are shown in Fig.3, shown by the logarithm intensity vs scan depth (pixels). In which the red solid line is the theory standard used for fitting scattering coefficients and anisotropy factors, the black solid line is for fitting scattering coefficients, absorption coefficients and anisotropy factors. The absorption coefficient is significantly lower than the scattering coefficient[20]. So the absorption coefficient is neglected for tissue; and the star dots are the fitting dots of OCT data, the fitting values are displayed at the bottom. It can be seem that star curve can be described by red solid line; and the error value is acceptable.

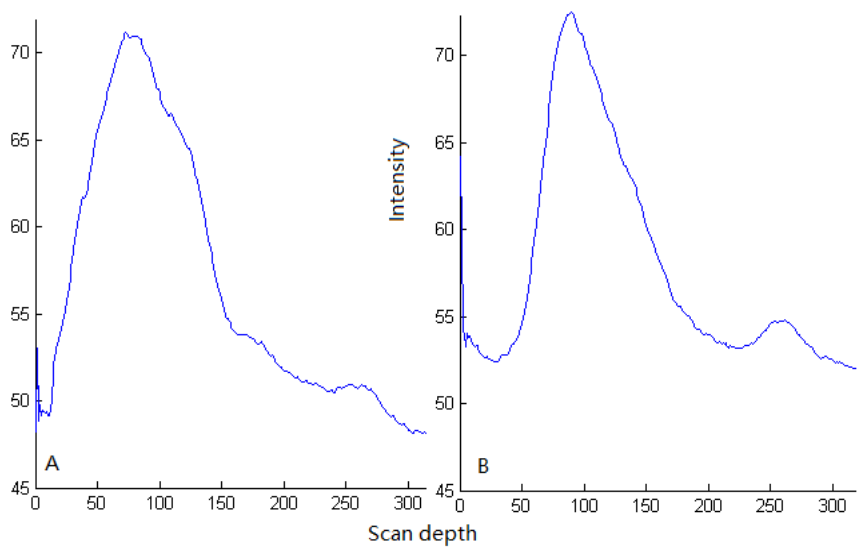

Fig.2: The averaged a-scan lines from normal(A) and cancer tissue(B) fitting by 350 pixels region of the decay slope.

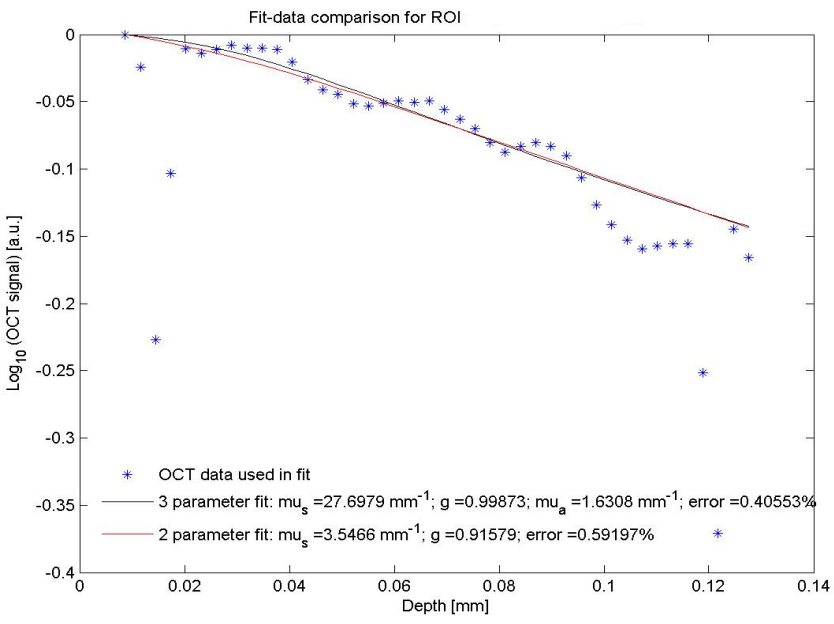

Fig.3: The representative plots of fitting scattering coefficient and anisotropy factor from certain region of interest (ROI).

The box-plots of median and interquartile range (IQR) fitting scattering coefficients and anisotropy factors for epithelium and lamina propria of normal and cancer tissue are shown in Fig.4, respectively. The median scattering coefficients of epithelium are 2.2 mm^{-1} (IQR 1.5 to 2.5 mm^{-1}) for normal versus 3.8 mm^{-1} (IQR 2.0 to 3.3 mm^{-1}) for cancer tissue, (Fig.4A); of lamina propria are 2.9 mm^{-1} (IQR 1.5 to 2.5 mm^{-1}) for normal versus 1.3 mm^{-1} (IQR 1.2 to 12 mm^{-1}) for cancer tissue, (Fig.4B);and anisotropy factors of epithelium are 0.91 (IQR 0.9 to 0.93) versus 0.91 (IQR 0.88 to 0.97) for normal and cancer tissue (Fig.4C); of lamina propria are 0.98 (IQR 0.94 to 0.99) for normal versus 0.98 (IQR 0.96 to 0.99) for cancer (Fig.4D), respectively. Where horizontal lines represent median values, boxes indicate IQRs, and error bars indicate the ranges.

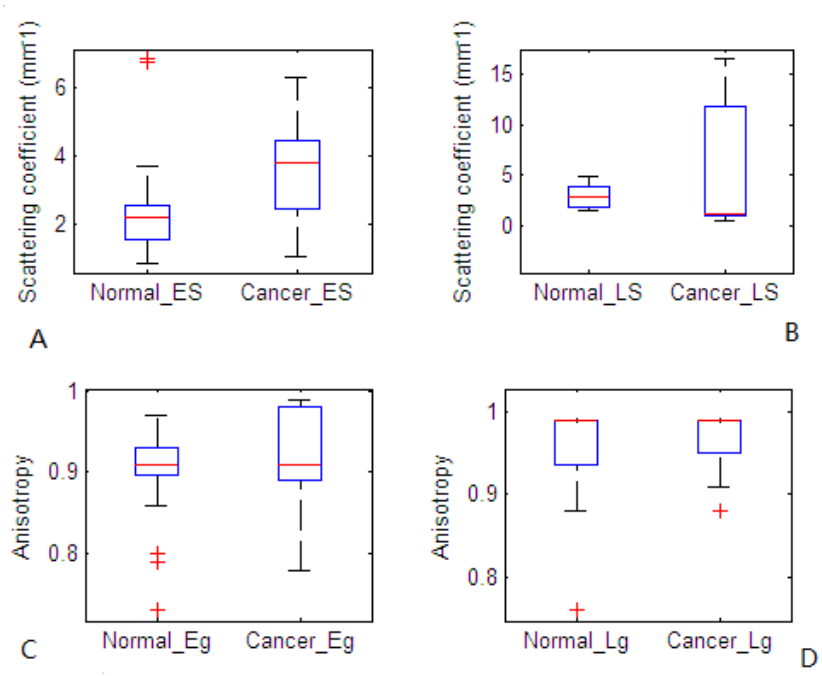

Fig.4: The box-plots of median and interquartile range (IQR) fitting scattering coefficients and anisotropy factors for epithelium and lamina propria of normal and cancer tissue.

Discussion

Optical coherence tomography (OCT) can function as a type of “optical biopsy”, enabling visualization of tissue microstructure with a resolution approaching that of histology, but without the need for tissue excision and processing[21]. OCT image of normal mucosa appears clearly layered image and the fitting optical parameters show the different values perhaps for the different refractive index caused by the different component. As we know, nasopharyngeal mucosa is composed of epithelium and lamina

propria[22]. The epithelium covers the surface of the nasopharynx, chromatin and protein are the main components of the epithelium; the cytoplasm contains a wealth of mitochondria and free ribosome. While the lamina propria is composed of connective tissue, there are abundant collagen fibers and elastic fibers, and there are many blood vessels and lymphatic vessels. According to the Fig.4, the fluctuation of optical parameters of cancer is larger than normal. With the development of the pathology, malignant cells display an increased number, larger and more irregularly shaped nuclei with a higher refractive index and more active mitochondria[23], the component distribution is not homogeneous any more. The values can aid to diagnosis the cancer from the normal tissue. However, the effective anisotropy factor demonstrates no significant difference between normal and cancer, perhaps because the geff of the fibrocalcific and fibrous lesions were correlated with the μ_s and Δn properties, respectively. The anisotropy factors of normal and cancer are larger than 0.8, which corresponds that tissue is generally considered to be highly forward scattering ($g > 0.8$) [24]. Anisotropy factors of 0.9 for tissue are very high because no correction of the OCT signal for the depth of focus of the sample arm optics and the focus position in the tissue[25,26].

Conclusion

In conclusion, OCT imaging has the potential be a valuable tool in detecting mucosa abnormalities with the morphology, because the epithelial layer, lamina propria, and basement membrane layer in mucosa has the different optical properties. The quantitative fitting values of scattering coefficient in mucosa show the difference between the normal and cancer, which can offer the reference for the diagnosis.

Acknowledgements

This work was funded by the National Natural Science Foundation of China (31200629), and the Shenzhen Science and Technology Innovation Committee (JCYJ20150417094158018, JCYJ20150417094158026), (lg201419)

References

[1] Wei KR, Zheng RS, Zhang SW, et al. Nasopharyngeal carcinoma incidence and mortality in China in 2010. Chin J Cancer. 2014; 33(8): 381–387.

[2] Ho FC, Tham IW, Earnest A, et al. Patterns of regional lymph node metastasis of nasopharyngeal carcinoma: a meta-analysis of clinical evidence. BMC Cancer. 2012; 12: 98.

[4] Wei WI, Sham JS. Nasopharyngeal carcinoma. Lancet. 2005; 365(9476): 2041–2054.

[5] Huang D, Swanson EA, Lin CP, et al. Optical coherence tomography. Science. 1991; 254(5035): 1178–1181.

[6] Raghunathan R, Singh M, Dickinson ME, et al. Optical coherence tomography for embryonic imaging: a review. J Biomed Opt. 2016; 21(5): 50902.

[7] Mogensen M, Thrane L, Jørgensen TM, et al. OCT imaging of skin cancer and other dermatological diseases. J Biophotonics. 2009; 2(6–7): 442–451.

[8] Fujimoto JG. Optical coherence tomography for ultrahigh resolution in vivo imaging. Nat Biotechnol. 2003; 21(11): 1361–1367.

[9] Pan Y, Lavelle JP, Bastacky SI, et al. Detection of tumorigenesis in rat bladders with optical coherence tomography. Med Phys. 2001; 28(12): 2432–2440.

[10] Qi X, Sivak MV, Isenberg G, et al. Computer-aided diagnosis of dysplasia in Barrett's esophagus using endoscopic optical coherence tomography. J Biomed Opt. 2006; 11(4): 044010.

[11] Goldberg BD, Iftimia NV, Bressner JE, et al. Automated algorithm for differentiation of human breast tissue using low coherence interferometry for fine needle aspiration biopsy guidance. J Biomed Opt. 2008; 13(1): 014014.

[13] Zakharov V P, Bratchenko I A, Myakinin O O, et al. Multimodal diagnosis and visualisation of oncologic pathologies. Quantum Electronics. 2014; 44(8): 726–731.

[14] Levitz D, Thrane L, Frosz M, et al. Determination of optical scattering properties of highly-scattering media in optical coherence tomography images. Opt Express. 2004; 12(2): 249–259.

[15] Thrane L, Yura HT, Andersen PE. Analysis of optical coherence tomography systems based on the extended Huygens-Fresnel principle. J Opt Soc Am A Opt Image Sci

Vis. 2000; 17(3): 484–490.

[17] Wang K, Ding Z, Wang L. Determining tissue optical properties by optical coherence tomography. Acta Photonica Sinica. 2008; 6534(3)：65340F–65340F–10.

[17] Wang K, Ding ZH, Wang L, Wang K, Ding ZH, Wang L, Measuring Tissue Optical Properties by Optical Coherence Tomography. Acta Photonica Sinica. 2008; 37(3): 523–527.

[20] Qu J, Macaulay C, Lam S, et al. Optical properties of normal and carcinomatous bronchial tissue. Appl Opt. 1994; 33(31): 7397–7405.

[21] Liu L, Gardecki JA, Nadkarni SK, et al. Imaging the subcellular structure of human coronary atherosclerosis using micro-optical coherence tomography. Nat Med. 2011; 17(8): 1010–1014.

[23] Wessels R, De Bruin DM, Faber DJ, et al. Optical biopsy of epithelial cancers by optical coherence tomography (OCT). Lasers Med Sci. 2014; 29(3): 1297–1305.

[25] van Leeuwen T G, Faber D J, Aalders M C. Measurement of the axial point spread function in scattering media using single-mode fiber-based optical coherence tomography. IEEE Journal of Selected Topics in Quantum Electronics. 2003; 9(2): 227–233.

[26] Faber DJ, van der Meer FJ, Aalders MCG, et al. Quantitative measurement of attenuation coefficients of weakly scattering media using optical coherence tomography. Optics Express. 2004; 12(19): 4353.